Applying closed-loop equations for kinematic analysis of an eight-bar walking mechanism

Dang Anh Tuan*, Nguyen Thi Thu Linh

Faculty of International Training, Thai Nguyen University of Technology, 666 3/2 Road, Thai Nguyen City, Thai Nguyen, Vietnam.
*Corresponding author: anhtuanck@tnut.edu.vn
Received 1 Aug. 2024; Revised 5 Nov. 2024; Accepted 15 Nov. 2024; Published 6 Dec. 2024.
DOI: https://doi.org/10.54939/1859-1043.j.mst.FEE.2024.157-163

ABSTRACT

Bionic mechanisms are used in constructing robotic systems that perform complex tasks similar to the movement of animals. With advancements in scientific research and breakthroughs in simulation techniques and computational methods, the design of these systems has become increasingly detailed and refined. This paper proposes using the closed-loop method to analyze the operational characteristics of a wheelless walking mechanism designed to traverse complex terrains. In addition to evaluating fundamental factors affecting system operation, the study determines kinematic parameters such as leg trajectory, movement velocity, and tilt angle. The results demonstrate the effectiveness of numerical methods in analyzing and simulating real-world systems, thus extending the use of computational tools for analyzing similar linkages.

Keywords: Walking mechanism, eight-bar linkage, Kinetic Analysis, Kinetic Inversion, close-loop equation.

1. INTRODUCTION

With the development of science and technology, human research on nature, specifically the original existing patterns in the natural world, has increased. The growth of the Industrial Revolution has accelerated the migration of information technology and advanced techniques, making the study of biological systems, which aims to replicate and simulate the structures, functions, and behaviors of living organisms for engineering applications, a major field.

Specifically, natural structures such as honeycombs, spider webs, and vein nets on leaves are analyzed, simulated, and applied to construction, allowing for the creation of sustainable and efficient architectural designs [1-5]. Based on natural phenomena, many simulation, optimization, and control algorithms have been developed and applied. To optimize technical and economic problems, the Genetic Algorithm, based on natural evolution processes, has been proposed and developed [6, 7]. By observing the social behaviors of flocks of birds or schools of fish interacting while searching for food, Particle Swarm Optimization (PSO), which is still considered one of the best optimization algorithms due to its ability to produce flexible optimum solutions, was introduced [8, 9]. In addition to bionic models and algorithms, mechanical systems that mimic the movement of living organisms have also been researched and developed [10-12]. These systems improve the efficiency and functionality of technical systems and expand the understanding of biological structures and their application to solving real-world problems. To simulate movement on uneven terrain, robot systems without wheels have been used, such as the Jansen linkage mimicking the structure of animal legs, or the Klann linkage simulating the movement of insects. Although the construction is simple, every part is connected by pin joints, meaning that the dimensions of the component links affect the movement of others. Therefore, determining the relationships between these components is important. This not only aids in understanding the kinematics and operational methods of the linkages but also helps in applying optimization algorithms to enhance the system's overall efficiency. However, because of the complex kinematic properties, previous research on these linkages has primarily focused on adjusting a few basic parameters for evaluation, and a comprehensive understanding of the kinematics and kinetics of these mechanisms has not been extensively conducted.

This study proposes using closed-loop equations to analyze the operation of a new type eight-bar leg mechanism. Besides constructing a general equation for the movement of the leg, the study uses kinetic inversion to determine the movement of the mechanism and reaction on the component joints. The study also determines systematic parameters such as foot trajectory, tilting angle, and moving velocity.

2. KINEMATIC ANALYSIS

The proposed linkage is a variable of the Ghassaei mechanism, and consists of eight links, as depicted in figure 1. Unlike the original design, which has two plates at the ground pivot O_4 and the foot at point E, the proposed structure integrates a bent frame and extends link 7 to create a point-contact leg. This adjustment reduces the working range for the linkage while maintaining a smooth and precise motion path across the mechanism. In this configuration, driving link O_2A rotates with a constant speed ω_2. The frame O_2O_4 is fixed to the body, anchoring points O_2 and O_4 as grounded rotating joints. Since these joints directly connect to couple links 3-4 and 5-6, the positions of joints B and C are determined through the four-bar linkages O_2O_4AB and O_2O_4AC; and from the position of the joints C and D on the BO_4D bar, the position of point E in the four-bar linkage O_4CDE can be calculated. Subsequently, the position of foot F then can be derived based on points C and E. To determine the positions of the component frames, closed-loop equations are used, which can be divided into three groups (see figure 1b). By solving the position equation for each loop, the movement of the foot can be tracked.

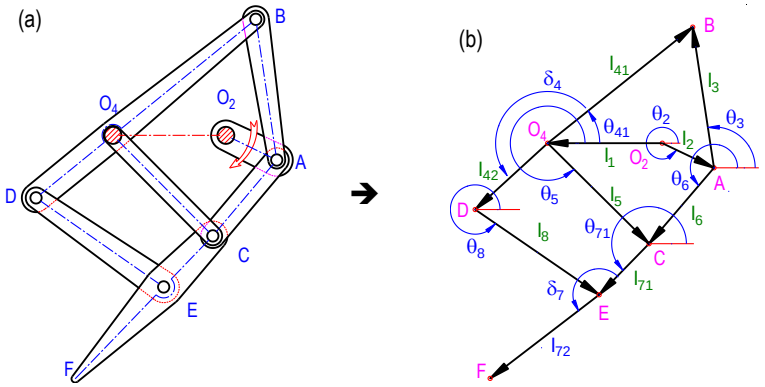

Figure 1. *Structure of the linkage: (left) theoretical model and (right) closed-loop shaped.*

For the first loop equation: $\vec{l_2}+\vec{l_3}=\vec{l_1}+\vec{l_{41}}$

Project equation into x- and y-direction:

$$\begin{cases} l_1\cos\theta_1 - l_2\cos\theta_2 + l_{41}\cos\theta_{41} = l_3\cos\theta_3 \\ l_1\sin\theta_1 - l_2\sin\theta_2 + l_{41}\sin\theta_{41} = l_3\sin\theta_3 \end{cases} \quad (1)$$

Based on this system, the position of link 41 can be determined as:

$$\theta_{41} = -\arcsin\left[\frac{l_1^2+l_2^2+l_{41}^2-l_3^2-2l_1l_2\cdot\cos(\theta_1-\theta_2)}{2l_{41}\sqrt{l_1^2+l_2^2-2l_1l_2\cos(\theta_1-\theta_2)}}\right] - \arctan\left(\frac{l_1\cos\theta_1-l_2\cos\theta_2}{l_1\sin\theta_1-l_2\sin\theta_2}\right) \quad (2)$$

For the second loop: $\vec{l_2}+\vec{l_6}=\vec{l_1}+\vec{l_5}$

$$\begin{cases} l_1\cos\theta_1 - l_2\cos\theta_2 + l_5\cos\theta_5 = l_6\cos\theta_6 \\ l_1\sin\theta_1 - l_2\sin\theta_2 + l_5\sin\theta_5 = l_6\sin\theta_6 \end{cases} \quad (3)$$

The position of links 5 and can be determined as:

$$\theta_5 = \arcsin\left[\frac{l_1^2 + l_2^2 + l_5^2 - l_6^2 - 2l_1l_2 \cdot \cos(\theta_1 - \theta_2)}{2l_5\sqrt{l_1^2 + l_2^2 - 2l_1l_2\cos(\theta_1 - \theta_2)}}\right] - \arctan\left(\frac{l_1\cos\theta_1 - l_2\cos\theta_2}{l_1\sin\theta_1 - l_2\sin\theta_2}\right) \quad (4)$$

For the third loop: $\overrightarrow{l_{42}} + \vec{l_8} = \vec{l_5} + \overrightarrow{l_{71}}$

$$\begin{cases} l_5\cos\theta_5 - l_{42}\cos\theta_{42} + l_{71}\cos\theta_{71} = l_8\cos\theta_8 \\ l_5\sin\theta_5 - l_{42}\sin\theta_{42} + l_{71}\sin\theta_{71} = l_8\sin\theta_8 \end{cases} \quad (5)$$

Since $\theta_{42} = \theta_{41} + \delta_4$, the position of link 71 and can be withdrawn as:

$$\theta_{71} = \arcsin\left[\frac{l_5^2 + l_{42}^2 + l_{71}^2 - l_8^2 - 2l_5l_{42}\cos(\theta_5 - \theta_{41} - \delta_4)}{2l_{71}\sqrt{l_5^2 + l_{42}^2 - 2l_5l_{42}\cos(\theta_5 - \theta_{41} - \delta_4)}}\right] - \arctan\left[\frac{l_5\cos\theta_5 - l_{42}\cos(\theta_{41} + \delta_4)}{l_5\sin\theta_5 - l_{42}\sin(\theta_{41} + \delta_4)}\right] \quad (6)$$

The position of the foot F then can be calculated as: $\overrightarrow{O_2F} = \vec{l_1} + \vec{l_5} + \overrightarrow{l_{71}} + \overrightarrow{l_{72}}$

Project equation into x- and y-direction:

$$\begin{cases} x_F = l_1\cos\theta_1 + l_5\cos\theta_5 + l_{71}\cos\theta_{71} + l_{72}\cos(\theta_{71} - \pi + \delta_7) \\ y_F = l_1\sin\theta_1 + l_5\sin\theta_5 + l_{71}\sin\theta_{71} + l_{72}\sin(\theta_{71} - \pi + \delta_7) \end{cases} \quad (7)$$

To traverse complex terrains, the system includes auxiliary legs divided into left and right branches, as shown in figure 2a, with the drive source (motor) located at point M. The motor transmits motion to the mechanisms on both sides through the gear sets Z_1-Z_2-Z_2'. The gears are arranged to ensure that the linkages on both sides rotate with the same speed and direction ($n_2 = n_2$'). This makes the movement characteristics of the left-side mechanism differ from those of the original right-side mechanism, indicating that the kinematic parameters of the component links on each side must be individually calculated. Additionally, since the linkages are allowed to rotate with different initial angles, the system can be arranged so that the feet alternatively make contact with the ground, ensuring stability and balance for the system. Figure 2b presents the structure of the system in vector form. The angular positions of component links in the right-side linkage can be calculated as a function of γ_2 (angle of driver link on the left-side branch).

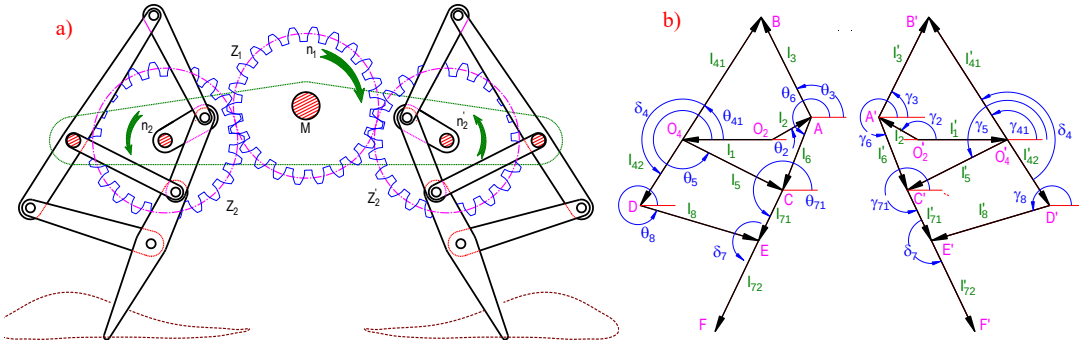

Figure 2. *Using gears to drive the legs and representing the system in vector form.*

The position of the foot F' then can be presented as:

$$\begin{cases} x_{F'} = x_{O_2O_2'} + l_1\cos\gamma_1 + l_5\cos\gamma_5 + l_{71}\cos\gamma_{71} + l_{72}\cos(\gamma_{71} + \pi - \delta_7) \\ y_{F'} = y_{O_2O_2'} + l_1\sin\gamma_1 + l_5\sin\gamma_5 + l_{71}\sin\gamma_{71} + l_{72}\sin(\gamma_{71} + \pi - \delta_7) \end{cases} \quad (8)$$

To ensure that the legs on the same side of the mechanism make contact with the ground in turn, offset angles δ_1 and δ_2 between the driver links of the linkages must be selected. This allows when one foot raises to a higher height, the other feet are at their lowest elevation, making contact with the ground. Similarly, for the linkages on the other side, when one of the feet is in contact with the ground, the others are in the raised position, allowing the robot to perform a forward-reaching motion for walking or overcoming obstacles, as presented in figure 3.

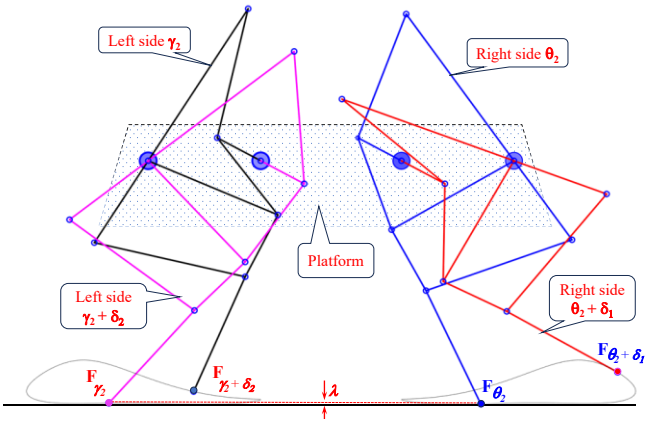

Figure 3. *The legs are arranged offset to ensure the feet always in contact with the ground.*

For the whole system to remain stable during the movement process and maintain balance for the body, two more pairs of legs will be used (to increase the contact point between the system and the ground). When the system operates, the foot with a lower height will touch the ground, while the others rise in the air. The feet in contact with the ground act as pin joints, moving the whole mechanism forward (or backward). The difference in driver angles of the linkages is calculated to ensure that as one set of feet lifts off, the other feet in the air will contact the ground, effectively switching their roles as ground-contact points. The legs touching the ground will be determined according to the following expression:

$$Right\_foot = \begin{cases} F_{\gamma_2} & \text{if } y\left(F_{\gamma_2}\right) < y\left(F_{\gamma_2+\delta_2}\right) \\ F_{\gamma_2+\delta_2} & \text{if } y\left(F_{\gamma_2}\right) \geq y\left(F_{\gamma_2+\delta_2}\right) \end{cases} \tag{9}$$

$$Left\_foot = \begin{cases} F_{\theta_2} & \text{if } y\left(F_{\theta_2}\right) < y\left(F_{\theta_2+\delta_1}\right) \\ F_{\theta_2+\delta_1} & \text{if } y\left(F_{\theta_2}\right) \geq y\left(F_{\theta_2+\delta_1}\right) \end{cases} \tag{10}$$

The tilt angle λ between the feet will accordingly determine the platform's oscillating angle:

$$\lambda = \arctan\left|\frac{y_{Right\_foot} - y_{Left\_foot}}{x_{Right\_foot} - x_{Left\_foot}}\right| \tag{11}$$

To determine the system's velocity, specifically velocities at the contact points between the feet and the ground, those of component links must be determined. By differentiating equations (1), (3), and (5), the angular velocities of the links are obtained and can be calculated as:

$$\omega_3 = \frac{l_2\omega_2 \sin\left(\theta_2 - \theta_{41}\right)}{l_3 \sin\left(\theta_{41} - \theta_3\right)} \qquad \omega_4 = \frac{l_2\omega_2 \sin\left(\theta_2 - \theta_3\right)}{l_{41} \sin\left(\theta_{41} - \theta_3\right)} \qquad \omega_6 = \frac{l_2\omega_2 \sin\left(\theta_2 - \theta_5\right)}{l_6 \sin\left(\theta_5 - \theta_6\right)}$$

$$\omega_5 = \frac{l_2\omega_2 \sin\left(\theta_2 - \theta_6\right)}{l_5 \sin\left(\theta_5 - \theta_6\right)} \qquad \omega_7 = \frac{l_{42}\omega_4 \sin\left(\theta_{41} + \delta_4 - \theta_8\right) - l_5\omega_5 \sin\left(\theta_5 - \theta_8\right)}{l_{71} \sin\left(\theta_{71} - \theta_8\right)} \tag{12}$$

And the velocity of the foot F and F' are determined using the equation:

$$\begin{cases} V_{Fx} = l_5\omega_5 \cos\theta_5 + l_{71}\omega_7 \cos\theta_{71} + l_{72}\omega_7 \cos\left(\theta_{71} - \pi + \delta_7\right) \\ V_{Fy} = l_5\omega_5 \sin\theta_5 + l_{71}\omega_7 \sin\theta_{71} + l_{72}\omega_7 \sin\left(\theta_{71} - \pi + \delta_7\right) \end{cases} \quad (13)$$

$$\begin{cases} V_{F'x} = l_5\omega_5' \cos\gamma_5 + l_{71}\omega_7' \cos\gamma_{71} + l_{72}\omega_7' \cos\left(\gamma_{71} + \pi - \delta_7\right) \\ V_{F'y} = l_5\omega_5' \sin\gamma_5 + l_{71}\omega_7' \sin\gamma_{71} + l_{72}\omega_7' \sin\left(\gamma_{71} + \pi - \delta_7\right) \end{cases} \quad (14)$$

The velocity of the platform is then determined by the velocities of the contact points of the feet to the ground. If there is a difference in velocity between the two sides, a slipping phenomenon will occur, affecting the system's performance. Alternatively, we can take the average velocity of both feet F and F' (assuming the system operates in an ideal environment), meaning:

$$V_{platform\_x} = \frac{V_{F'x} + V_{Fx}}{2} \quad and \quad V_{platform\_y} = \frac{V_{F'y} + V_{Fy}}{2} \quad (15)$$

3. RESULT AND DISCUSSION

By using the try-and-error method, a complete model of the system is obtained, with detailed dimensions are $\delta_1 = 180°$, $\delta_4 = 170°$, $\delta_7 = 183.6°$, $l_1 = 40$, $l_2 = 17.5$, $l_3 = 47.5$, $l_{41} = 65$, $l_{42} = l_6 = 35$, $l_5 = 50$, $l_{71} = 25$, $l_{72} = 45$, $l_8 = 55$ mm and $O_2O_2' = 100$ mm. The trajectories of feet F and F' are also determined, as shown in figure 4.

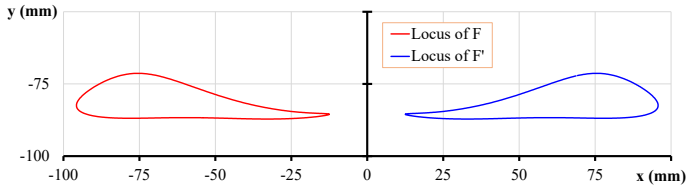

Figure 4. *Trajectories of the feet F and F'.*

To reduce the number of legs while ensuring that at least three feet touch the ground to keep the system balanced, the positions of the legs are modified to improve their stability. According to equation (9), by adjusting the offset angle δ_1 between the same-side linkage, specifically comparing the y-coordinates of the feet from the same side, the linkages whose feet contact the ground at different times can be determined. Figure 5 illustrates the real position of the ground-touching leg for different values of δ_1. It can be seen that when $\delta_1 = 180°$, the variation in distances between the leg and the motor (or platform) is minimized. For $\delta_1 \neq 180°$, there are situations where the legs touching the ground simultaneously, or both of them are in the raised state (meaning the platform must be lowered for the feet touching the ground), causing instability for the platform.

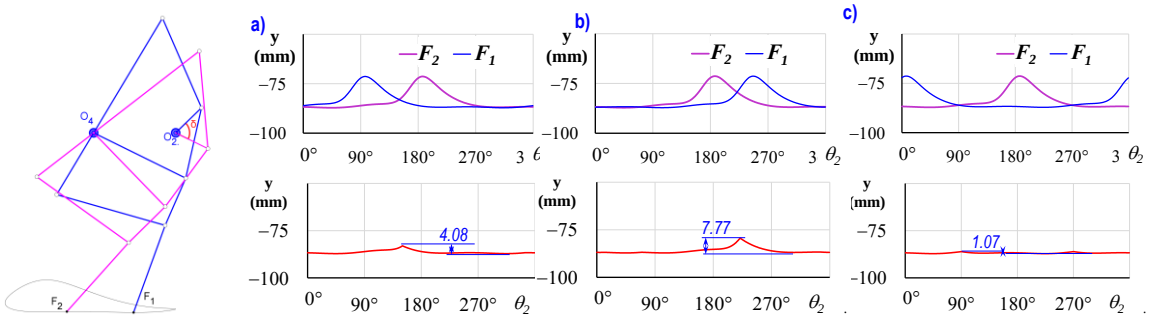

Figure 5. *Select the appropriate value of difference angles δ_2: position of the foot that in contact with the ground and the smooth of the trajectories where $\delta_2 = 60°$(a), $\delta_2 = 90°$(b) and $\delta_2 = 180°$(c).*

To calculate the platform oscillation, the difference in the initial angle between the cranks is analyzed. Since the alignment of the platform depends on the position of the feet, even a small difference in height between the legs impacts the system's stability. Figure 6 presents the diagram comparing the positions of the feet on the left- and the right side (using $\delta_1 = \delta_2 = 180°$) that touch the ground over time and the swing angle λ of the platform, using equation (11).

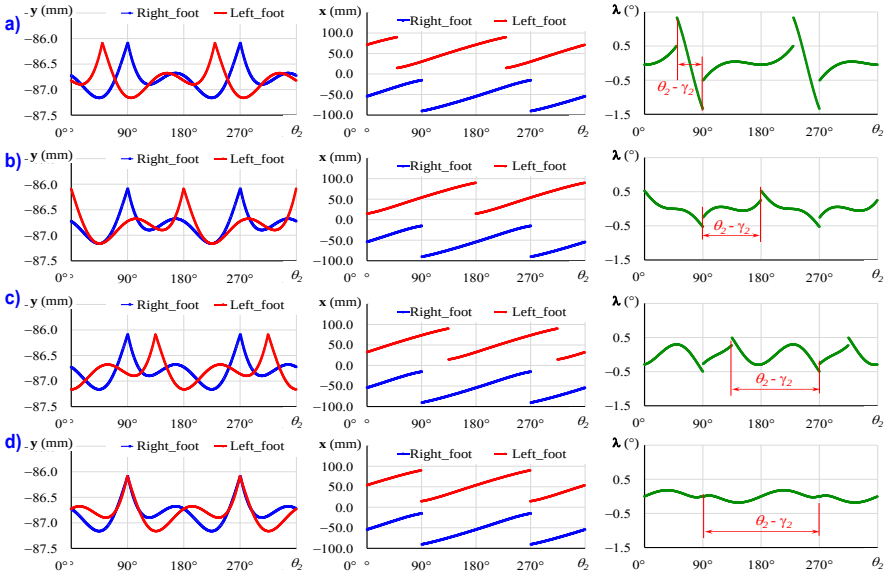

Figure 6. *Position of the grounded feet in both side linkages and the swing angle of the platform with $\delta_1 = \delta_2 = 180°$, $\theta_2 - \gamma_2 = 45°$ (a), $\theta_2 - \gamma_2 = 90°$ (b), $\theta_2 - \gamma_2 = 135°$ (c) and $\theta_2 - \gamma_2 = 180°$ (d).*

The figure also indicates that the higher the discrepancy between driver links, the greater of platform's oscillation. The feet change their contact state (touching the ground or lifting on one side, or both sides), which alters the distance between the contact points and indirectly causes the sudden changes in the swing angle of the platform. It is noted that in the case $-180° < \psi = \theta_2 - \gamma_2 < 0°$, the equation (11) about the inversion angle l will also give the same result as in the case $\psi + 180°$. With the selected linkage dimensions as designed, it is crucial to precisely adjust the positions the driver links (the offset angles δ_1, δ_2 of the linkage from the same sides, and the offset between the branches θ_2-γ_2) to always be 180°. This configuration ensures the smoothest movement of the mechanism with the smallest value of λ. Given the crank's rotational speed of $\omega_2 = 60$ rpm, the velocities of the platform can be calculated by combining the velocities of the legs from both sides, as presented in figure 7. It is clear that the y-direction component of the average velocity is smaller than that in the x-direction. One factor is that the movement of the feet in the ground is quite flat (the trajectory is mainly horizontal with a small curve up). The fluctuating velocities also indicate that the system is not moving constantly. Even when operating on a flat surface, it still creates vibrations in both directions for the platform during movement, increasing the impact and collision effects between parts and the ground.

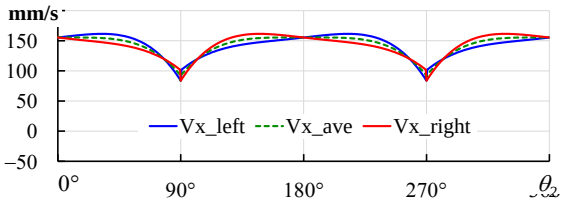

Figure 7. *Velocities of the feet F and of the whole mechanism in one cycle of driver link θ_2.*

4. CONCLUSIONS

This paper proposes a method to calculate and analyze the operation of an eight-bar walking mechanism. Different from solving by graphing method, the calculation using algebra equation to assist the calculation process can be done and integrated with numerical software to acquire results. Based on the movement of the robot legs, the locus of the feet, the tilted angle, and the translation velocity of the platform are determined. Since the calculation can be solved by substituting dimensions of component links into the equations, this method proposes a simple approach to designing complex linkages and optimizing them to improve efficient operation.

REFERENCES

[1]. Su, I., Narayanan *et al.*, *"In situ three-dimensional spider web construction and mechanics,"* Proceedings of the National Academy of Sciences, Vol. 118, no. 33, e2101296118, (2021).

[2]. Krink, Thiemo, and Fritz Vollrath. "*Analysing spider web-building behavior with rule-based simulations and genetic algorithms."* Journal of Theoretical Biology 185, no. 3: 321-331, (1997).

[3]. Zhang, Qiancheng, Xiaohu Yang, Peng Li, Guoyou Huang, Shangsheng Feng, Cheng Shen, Bin Han et al., "*Bioinspired engineering of honeycomb structure–Using nature to inspire human innovation*," Progress in Materials Science 74: 332-400, (2015).

[4]. Kuruppu, K. A. B. P., M. Nanthakumar, and K. Baskaran, *"Study on Honeycombs in Structural Concrete Elements,"* In 2022 Moratuwa Engineering Research Conference (MERCon), pp. 1-6. IEEE, (2022).

[5]. Liu, Yuan, Duyu Chen, Jianxiang Tian, Wenxiang Xu, and Yang Jiao. "*Universal Hyperuniform Organization in Looped Leaf Vein Networks*." Physical Review Letters 133, no. 2: 028401, (2024).

[6]. Tanese, R., *"Distributed genetic algorithms for function optimization,"* University of Michigan, (1989).

[7]. Moscato, P., *"On evolution, search, optimization, genetic algorithms and martial arts: Towards memetic algorithms,"* Caltech concurrent computation program, C3P Report, 826, 37, (1989).

[8]. Kennedy J., and Eberhart R.C., "*Particle swarm optimization*", Proceeding of the 1995 IEEE International Conference on Neural Networks, Perth, Australia, pp. IV: 1942-1948, (1995).

[9]. Wang, D., Tan, D., & Liu, L.. "*Particle swarm optimization algorithm: an overview*," Soft computing, 22: 387-408, (2018).

[10]. Ghassaei, Amanda, Professors Phil Choi, and Dwight Whitaker. "*The design and optimization of a crank-based leg mechanism*." Pomona, USA, (2011)..

[11]. Patnaik, Lalit, and Loganathan Umanand. "*Kinematics and dynamics of Jansen leg mechanism: A bond graph approach*." Simulation Modelling Practice and Theory 60: 160-169, (2016).

[12]. Dang, AT., Nguyen, DN., Nga, N.T.T., Linh, N.T.T. *"Analysis Rope Climbing Mechanism,"* Advances in Engineering Research and Application. ICERA 2021, (2022).

TÓM TẮT

Ứng dụng phương trình chuỗi động kín vào phân tích động học cho cơ cấu robot tám khâu

Các cơ cấu phỏng sinh học được dụng làm cơ sở chế tạo các hệ thống robot, bắt chước các cử động của động vật, nhằm thực hiện các chuyển động phức tạp. Bài báo này đề xuất sử dụng phương pháp chuỗi vector để phân tích các thông số làm việc của cơ cấu tám khâu, một dạng chân robot được sử dụng để di chuyển trên các địa hình phức tạp. Ngoài việc đánh giá các yếu tố cơ bản ảnh hưởng đến hoạt động của hệ thống, nghiên cứu còn xác định các thông số động học như quỹ đạo chân, vận tốc di chuyển và góc nghiêng của sàn. Kết quả cho thấy hiệu quả của các phương pháp số trong việc phân tích và mô phỏng các hệ thống thực tế, mở rộng việc sử dụng các công cụ tính toán để phân tích các cơ chế tương tự.

Từ khóa: Robot di chuyển; Cơ cấu tám khâu; Phân tích động học; Động học ngược; Phương trình chuỗi động kín.